

# Cardiomyocyte mitochondrial dynamic-related lncRNA 1 (CMDL-1) may serve as a potential therapeutic target in doxorubicin cardiotoxicity

Lynn Htet Htet Aung,<sup>1,2,4</sup> Xiatian Chen,<sup>1,4</sup> Juan Carlos Cueva Jumbo,<sup>3</sup> Zhe Li,<sup>1</sup> Shao-ying Wang,<sup>1</sup> Cheng Zhao,<sup>1</sup> Ziqian Liu,<sup>1</sup> Yin Wang,<sup>1</sup> and Peifeng Li<sup>1,2</sup>

<sup>1</sup>Center for Molecular Genetics, Institute of Translational Medicine, The Affiliated Hospital of Qingdao University, College of Medicine, Qingdao University, Qingdao 266000, Shandong, China; <sup>2</sup>Center for Bioinformatics, Institute of Translational Medicine, College of Medicine, Qingdao University, Qingdao 266000, Shandong, China; <sup>3</sup>School of Preclinical Medicine, Nanobody Research Center, Guangxi Medical University, Nanning 530021, China

**Doxorubicin (DOX)-induced cardiotoxicity has been one of the major limitations for its clinical use. Although extensive studies have been conducted to decipher the molecular mechanisms underlying DOX cardiotoxicity, no effective preventive or therapeutic measures have yet been identified. Microarray analysis showed that multiple long non-coding RNAs (lncRNAs) are differentially expressed between control- and DOX-treated cardiomyocytes. Functional enrichment analysis indicated that the differentially expressed genes are annotated to cardiac hypertrophic pathways. Among differentially expressed lncRNAs, cardiomyocyte mitochondrial dynamic-related lncRNA 1 (CMDL-1) is the most significantly downregulated lncRNA in cardiomyocytes after DOX exposure. The protein-RNA interaction analysis showed that CMDL-1 may target dynamin-related protein 1 (Drp1). Mechanistic analysis shows that lentiviral overexpression of CMDL-1 prevents DOX-induced mitochondrial fission and apoptosis in cardiomyocytes. However, overexpression of CMDL-1 cannot effectively reduce mitochondrial fission when Drp1 is minimally expressed by small interfering RNA Drp1 (siDrp1). Overexpression of CMDL-1 promotes the association between CMDL-1 and Drp1, as well as with phosphorylated (p-)Drp1, as evidenced by RNA immunoprecipitation analysis. These data indicate the role of CMDL-1 in posttranslational modification of a target protein via regulating its phosphorylation. Collectively, our data indicate that CMDL-1 may play an anti-apoptotic role in DOX cardiotoxicity by regulating Drp1 S637 phosphorylation. Thus, CMDL-1 may serve as a potential therapeutic target in DOX cardiotoxicity.**

## INTRODUCTION

Doxorubicin (DOX), an anthracycline chemotherapeutic agent, has been one of the widely used anti-cancer drugs for both children and adult patients. However, its therapeutic benefits and long-term usage are limited by the cumulative and dose-dependent cardiac toxicity ranging from trivial changes in myocardial structure and function to severe cardiomyopathy and congestive heart failure.<sup>1,2</sup>

Although extensive studies have been conducted to decipher the exact molecular mechanisms underlying DOX cardiotoxicity, so far, no effective preventive or therapeutic measures have been identified.<sup>3</sup> Several studies have evinced that DOX cardiotoxicity is associated with DNA damage, increase generation of reactive oxygen species (ROS), and mitochondrial dysfunction.<sup>4,5</sup> Despite the multiple signaling pathways involved in DOX cardiotoxicity, most of these mechanisms ultimately lead to the activation of apoptosis, contributing to the progressive loss of cardiac contractile function, and eventually heart failure.<sup>4,6</sup> Thus, in order to develop an effective preventative and therapeutic strategy that averts cardiotoxicity and preserves cardiac function during DOX treatment, it is critical to understand the molecular mechanism underlying the DOX-induced cardiomyocyte loss.

It is well established that mitochondrial morphology plays a critical role in cardiomyocyte apoptosis. Imbalance in mitochondrial fusion and fission is observed in various cardiovascular diseases, including cardiac ischemia, heart failure, and cardiomyopathies.<sup>7,8</sup> DOX cardiotoxicity is closely linked to mitochondrial dysfunction; dysfunctional mitochondrial fission and mitophagy are observed in DOX cardiotoxicity.<sup>9</sup> Dynamin-related protein 1 (Drp1), a large GTPase cytosolic protein, is responsible for outer mitochondrial membrane (OMM) fission. During mitochondrial fission, Drp1 is recruited to the OMM and forms a ring-like structure around the mitochondrial membrane, leading to constriction of the mitochondrial membrane.<sup>10</sup> Drp1 can be reversibly phosphorylated at its serine residues, and the localization or activation of cardiac Drp1 is strongly influenced by its phosphorylation status.<sup>11-13</sup> Phosphorylation of Drp1 at serine 637 prevents Drp1 translocation to mitochondria and inhibits

Received 27 March 2021; accepted 13 August 2021;  
<https://doi.org/10.1016/j.omtn.2021.08.006>

<sup>4</sup>These authors contributed equally

**Correspondence:** Lynn Htet Htet Aung, Center for Molecular Genetics, Institute of Translational Medicine, The Affiliated Hospital of Qingdao University, College of Medicine, Qingdao University, Qingdao 266000, Shandong, China.

**E-mail:** [lynnaung@qdu.edu.cn](mailto:lynnaung@qdu.edu.cn)



mitochondrial fission.<sup>13</sup> Din et al.<sup>14</sup> indicated that increased expression of serine/threonine-protein kinase Pim-1 in neonatal rat cardiomyocytes (NRCMs) prevented Drp1 translocation and subsequently inhibited mitochondrial fission and apoptosis, thereby reducing cardiac damage after ischemia injury. Therefore, understanding the molecular mechanism of how Drp1 function is regulated during DOX exposure is essential to ameliorate its cardiotoxic effect.

With the rapid advancement in high-throughput sequencing technologies, scientists continue to identify different forms of non-coding RNAs, which account for approximately 98% of the human genome.<sup>15</sup> Long non-coding RNAs (lncRNAs) are 200-nt-long non-coding RNA transcripts that are involved in the regulation of gene expression as well as gene function through diverse molecular mechanisms. Based on gene-regulating mechanisms, lncRNAs can be classified into four main categories, including signal, decoy, guide, and scaffold lncRNAs.<sup>15</sup> lncRNAs are dynamically expressed during different cellular developmental stages and cardiovascular pathologies, suggesting their potential to serve as biomarkers and therapeutic targets for various cardiovascular diseases.<sup>16,17</sup> Several recent studies have reported that lncRNAs can influence cardiac apoptosis via regulating mitochondrial dynamic pathways.<sup>18–20</sup> For example, cardiac apoptosis-related lncRNA (CARL) can prevent ischemia-induced mitochondrial fission and apoptosis by suppressing miR-539 activity, which promotes mitochondrial fission via inhibiting prohibitin-2 (Phb2) expression.<sup>18</sup> However, very little is known about the role of lncRNA in DOX-induced cardiac apoptosis.

Our study revealed a significant downregulation of cardiomyocyte mitochondrial dynamic-related lncRNA 1 (CMDL-1) expression in cardiomyocytes upon DOX exposure compared to untreated control (CT) samples, evidenced by both microarray and quantitative real-time PCR analyses. Functional enrichment analysis showed that the differentially expressed genes are enriched in cardiomyocyte hypertrophic pathways. CMDL-1 is located in proximity to the *Trpm-7* (transient receptor potential cation channel, subfamily M, member 7) kinase gene that can be transcribed into phosphorylating protein kinase. So far, the function and mechanism of CMDL-1 have not yet been reported. *In silico* and RNA immunoprecipitation (RIP) analysis results showed a likelihood of physical interaction between CMDL-1 and the mitochondrial fission factor Drp1. Therefore, we aimed to decipher the role of novel lncRNA CMDL-1 in DOX cardiotoxicity, focusing on its functional correlation with Drp1 phosphorylation.

## RESULTS

### Microarray profiling identified differentially expressed lncRNAs and mRNAs between DOX-exposed and control cardiomyocytes

We profiled the expression levels of genome-wide lncRNAs and mRNAs between DOX-exposed and control cardiomyocytes. All samples were prepared in triplicates, and the extracted RNAs from the pooled samples underwent microarray analysis. We compared the distributions of expression values for the samples after normalization using a boxplot (Figures 1A and 1B). In the lncRNA expres-

sion profiling data, a total of 7,788 lncRNAs expressed in cardiomyocytes were evaluated. A comparison of lncRNA expression levels between DOX-treated and untreated cardiomyocytes identified 2,190 differentially expressed lncRNAs, of which 1,059 were upregulated and 1,131 were downregulated (with the cutoff fold change  $\geq 2.0$ ,  $p < 0.05$ , Figures 1C and 1E). The most upregulated and downregulated lncRNAs were BC083885 (fold change of 64.698) and MRAK082686 (fold change of 148.554) in the DOX-exposed group, respectively. The top 20 dysregulated lncRNAs are shown in the Table S2.

In the mRNA expression profiling data, a total of 12,595 mRNAs expressed in cardiomyocytes were analyzed. A comparison of mRNA expression levels between DOX-treated and untreated cardiomyocytes identified 4,983 differentially expressed mRNAs, of which 2,316 were upregulated and 2,367 were downregulated (with the cutoff fold change  $\geq 2.0$ ,  $p < 0.05$ , Figures 1D and 1F). The most upregulated and downregulated mRNAs were GenBank: NM\_080411 (fold change of 173.456) and GenBank: NM\_001107944 (fold change of  $-188.323$ ), respectively. The top 20 dysregulated mRNAs are shown in Table S3. Hierarchical clustering analysis arranges samples into groups based on their expression levels, which allows us to hypothesize about the relationships among the samples (Figures 1C and 1D).

### GO and KEGG pathway analysis for differentially expressed mRNAs

Given that the function of lncRNAs may be related to the protein-coding genes, we evaluated the enrichment of mRNAs in biological processes, cellular components, and molecular functions by using Gene Ontology (GO) and Kyoto Encyclopedia of Genes and Genomes (KEGG) pathway analysis. GO analysis of relevant factors from downregulated mRNA transcripts showed them to be annotated to metabolic processes (Figure S1A), enriched in intracellular components (Figure S1C), and involved in protein binding function (Figure S1E). However, the upregulated mRNAs were found to be involved in glucocorticoid secretion processes (Figure S1B), mainly distributed in intracellular components (Figure S1D), and also annotated to protein binding function (Figure S1F).

KEGG pathway analysis offered a reliable way to identify the candidate biological pathways through which the lncRNAs interacted with mRNAs. The pathway analysis showed that downregulated mRNAs were involved in the mitogen-activated protein kinase (MAPK) signaling pathway, ubiquitin-mediated proteolysis, adrenergic signaling in cardiomyocytes, proteoglycans in cancer, hepatitis B, the transforming growth factor (TGF)- $\beta$  signaling pathway, microRNAs in cancer, renal cell carcinoma, basal transcription factors, and the cell cycle (Figure 2A). Pathways associated with synaptic vesicle cycle; lysosome, complement, and coagulation metabolism; arginine and proline metabolism; collecting duct acid secretion; leukocyte trans-endothelial migration; fructose and mannose metabolism; and hypertrophic cardiomyopathy were enriched by upregulated mRNAs (Figure 2B).

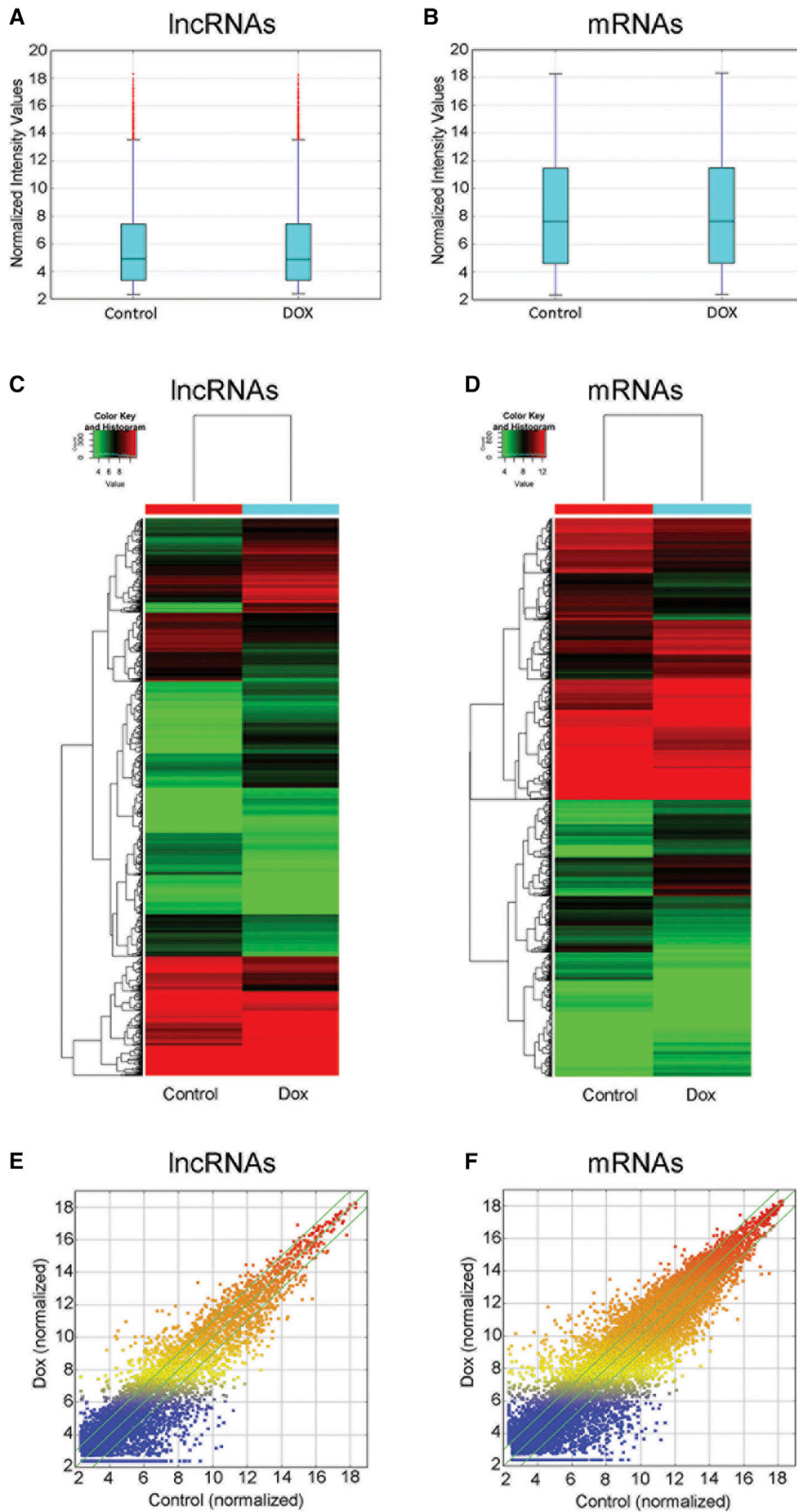


**Figure 1. Microarray profiling identified differentially expressed lncRNAs and mRNAs between doxorubicin (DOX)-exposed and control cardiomyocytes**

(A and B) Boxplot of all of the tested samples to quickly visualize the distribution for the lncRNA (A) and the mRNA (B) profiles. The samples in the dataset were normalized, and the medians of lncRNAs were close to 5 (A) and the medians of mRNA were close to 8 (B). (C and D) lncRNA and mRNA expression profiles between the untreated control and DOX-treated H9c2 cardiomyocytes. Hierarchical clustering analysis of gene expression levels between the two samples is shown. Cluster analysis indicated 2,190 lncRNAs (C) and 4,683 mRNAs (D). In the heatmap, red indicates upregulated expression and green indicates downregulated expression. (E and F) Scatterplots summarize lncRNA (E) and mRNA (F) expression variation between the two samples. The values of the x and y axes in the scatterplot are the averaged normalized signal values of the group ( $\log_2$  scaled). The green lines represent fold change (the default fold change given is 2.0).

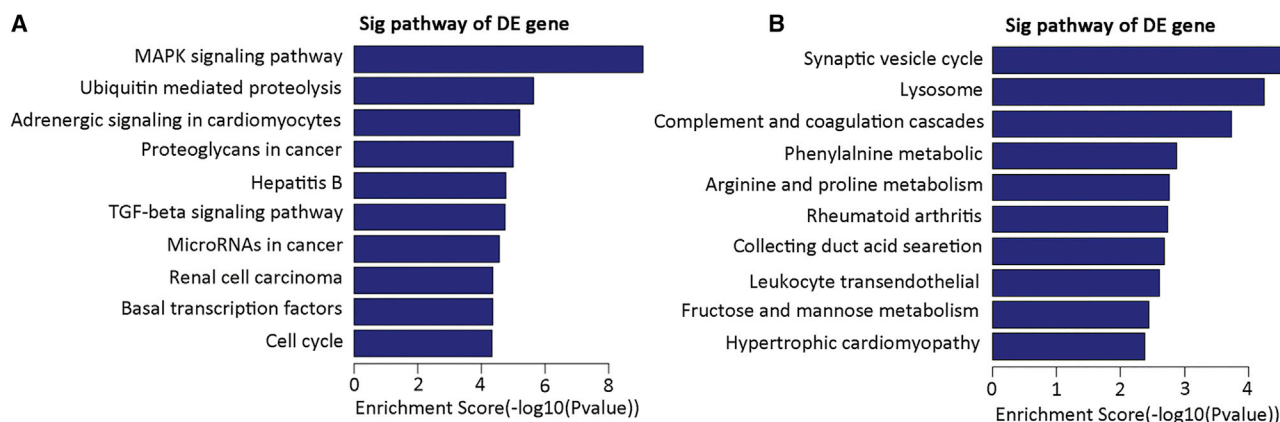


**Figure 2. KEGG analyses indicate that DOX can induce dysregulation of MAPK signaling and hypertrophic pathways in cardiomyocytes**

(A and B) KEGG pathways analysis of differentially expressed lncRNAs. The top 10 enrichment scores ( $-\log_{10}$ [p value]) of the significant enrichment pathway of downregulated (A) and upregulated pathways (B) are shown. A p value denotes the enrichment p value of the pathway ID used the Fisher's exact test. The enrichment score value of pathway ID is defined by ( $-\log_{10}$ [p value]). The lower the p value, the higher the enrichment score, and the more significant is the pathway enrichment.

#### Validation of expression levels of lncRNAs by quantitative real-time PCR

Expression levels of the selected top 20 lncRNAs (10 downregulated and 10 upregulated) detected in microarray analysis are shown in Figures 3A and 3B. The quantitative real-time PCR results showed the selected top 20 lncRNA expression differences in three paired DOX and control cardiomyocytes, which we used for microarray analysis (Figures 3C–3F). We analyzed the expression levels and fold change of the top 10 downregulated (Figures 3B and 3E) and upregulated (Figures 3D and 3F) lncRNAs. These findings indicated that the expression pattern of these top 20 differentially expressed lncRNAs were generally consistent between the microarray and quantitative real-time PCR results. Among those lncRNAs, MRAK164850, which we named CMDL-1, is the most significantly downregulated one in DOX-exposed cardiomyocytes as evidenced by both microarray and quantitative real-time PCR.

#### Sequence structure of CMDL-1

The full-length cDNA sequence of CMDL-1 is described in Figure 4A. CMDL-1 contained 39 exons and 38 introns, located at chromosome 3q36, and of 96% (query cover 49%) with Trpm-7, which can function as a kinase by phosphorylating itself or other substrates (Figure 4B). The secondary structure of CMDL-1 was predicted with minimum free energy (MFE) and minimum total base-paired distance to all structures in thermodynamics ensemble (centroid) models using the RNAfold web server (Figure 4C).

#### Overexpression of lncRNA CMDL-1 prevents DOX-induced mitochondrial fission and apoptosis in cardiomyocytes

We found that the expression of CMDL-1 in H9c2 cardiomyocytes is downregulated in a time-dependent manner upon DOX exposure (Figure 5A). To understand the role of CMDL-1 in DOX-induced cardiotoxicity, we overexpressed CMDL-1 in cardiomyocytes by infecting the cells with adenoviral overexpressing CMDL-1, and an empty

vector (EV) was used as a control (Figure 5B). Several studies have indicated that DOX can induce mitochondrial fission and apoptosis in cardiomyocytes.<sup>9,21,22</sup> To detect whether CMDL-1 can influence the cardiac mitochondrial fission, we induced CMDL-1 overexpression in cardiomyocytes as mentioned above and analyzed the mitochondrial morphology. As shown in Figures 5C and 5D, CMDL-1 overexpressed cardiomyocytes showed less mitochondrial fragmentation upon DOX exposure compared to negative and empty vector control groups. Next, to assess whether CMDL-1 can affect apoptosis, we detected the number of cells undergoing apoptosis using flow cytometry. Consistent with mitochondrial fission, cells with CMDL-1 overexpression showed a significant reduction in DOX-induced apoptosis (Figures 5E and 5F). These data suggest that overexpression of CMDL-1 ameliorates DOX-induced mitochondrial fission and apoptosis.

#### CMDL-1 regulates apoptosis via Drp1

It has been well established that mitochondrial fission is regulated by the mitochondrial fission proteins such as Drp1, mitochondrial fission 1 protein (Fis1), and mitochondrial fission factor (Mff).<sup>23,24</sup> To explore the downstream target of CMDL-1 in the mitochondrial fission pathway, we used an *in silico* approach with catRAPID to identify the potential interaction between CMDL-1 and the mitochondrial fission proteins, including Drp1, Fis1, and Mff, of which Drp1 showed a strong propensity of interaction with CMDL-1 (normalized score of 2.7). Next, we used the catRAPID fragment algorithm to predict the potential region of CMDL-1 that interacted with Drp1 and found that a protein region (511–602) of Drp1 and an RNA region (514–629) (5' region) of CMDL-1 possessed a strong interaction propensity (12.13) and high discriminative power (35) (Figures 6A and 6B).

We detected the expression levels of Drp1 and Trpm-7 upon DOX exposure and observed a time-dependent upregulation in their expression (Figure 6C). To understand the role of Drp1 in CMDL-1

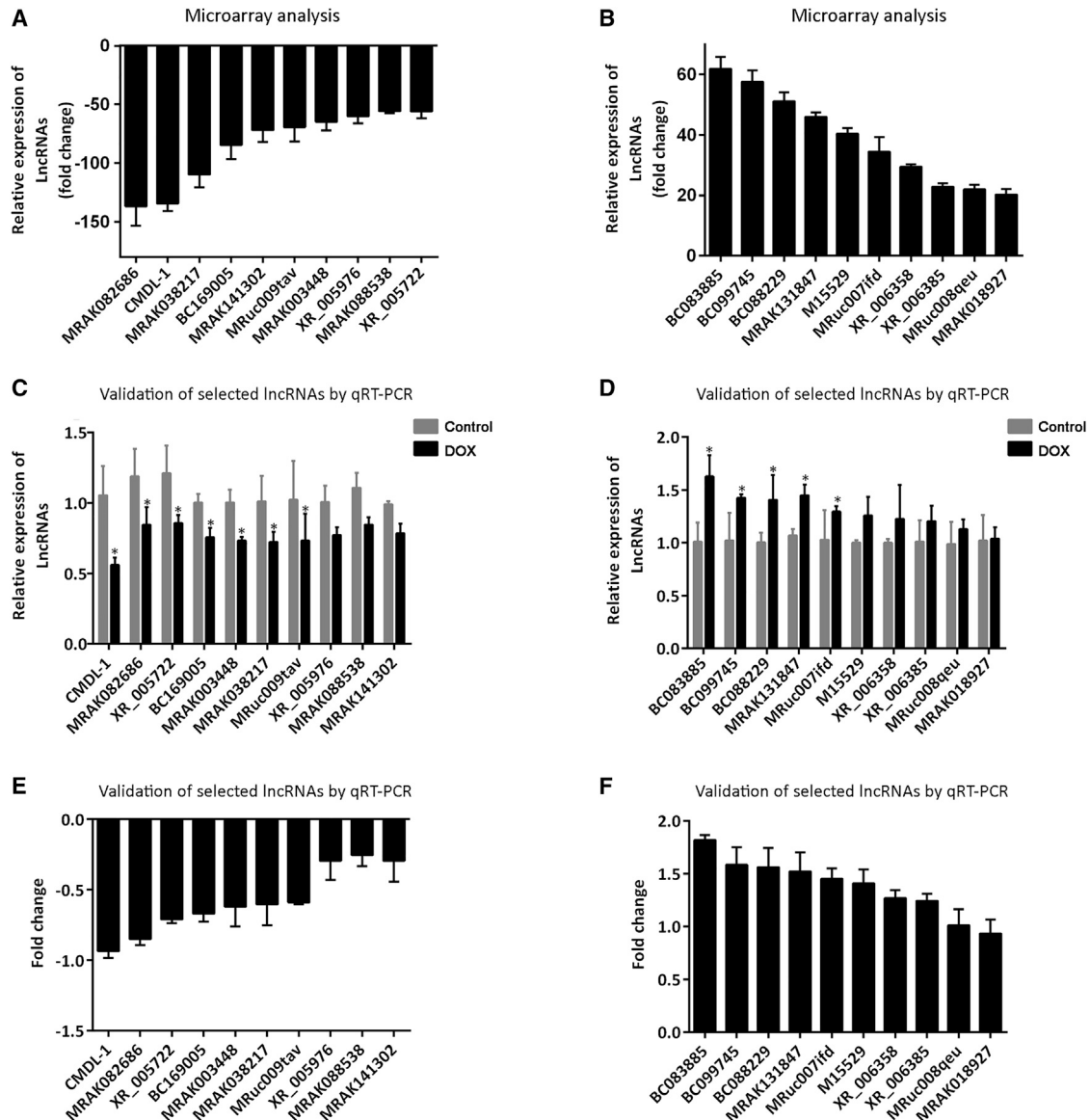


**Figure 3. CMDL-1 is the most significantly downregulated lncRNA in cardiomyocytes after DOX exposure**

(A and B) Top 10 differentially expressed lncRNAs analyzed by microarray analysis. Comparison of the consistently downregulated (A) and upregulated (B) lncRNAs in untreated control and DOX-treated samples ( $n = 3$ ) is shown. (C and D) Quantitative real-time PCR was used to validate downregulated (C) and upregulated (D) lncRNAs. (E and F) Fold change expression levels of quantitative real-time PCR validated downregulated (E) and upregulated (F) lncRNAs. Data are expressed as the mean  $\pm$  SEM. \* $p < 0.05$  compared to control samples as calculated by a two-sided Wilcoxon signed-rank test.

signaling, we detected the changes in Drp1 expression when CMDL-1 was overexpressed. Interestingly, we did not observe a significant reduction in Drp1 expression in cardiomyocytes overexpressing CMDL-1 (Figure 6D). Then, we hypothesized that if CMDL-1 exerts its function through Drp1, then when Drp1 is minimally expressed, the anti-mitochondrial fission effect of CMDL-1 overexpression should either be reduced or disappear. In Figures 6E and 6F, our results show that either CMDL-1 overexpression or Drp1 depletion significantly inhibits mitochondrial fission. However, the anti-mito-

chondrial fission effect of CMDL-1 was reduced when Drp1 was minimally expressed (Figures 6E and 6F), indicating that Drp1 is essential for CMDL-1 function. As expected, when Drp1 was minimally expressed, the anti-apoptotic effect of CMDL-1 was reduced (Figure 6G). Interestingly, although the knockdown of Drp1 suppressed the anti-mitochondrial fission and anti-apoptotic effects of CMDL-1, its effect was not that of complete inhibition, implying that CMDL-1 may regulate Drp1 function but not through affecting Drp1 expression.



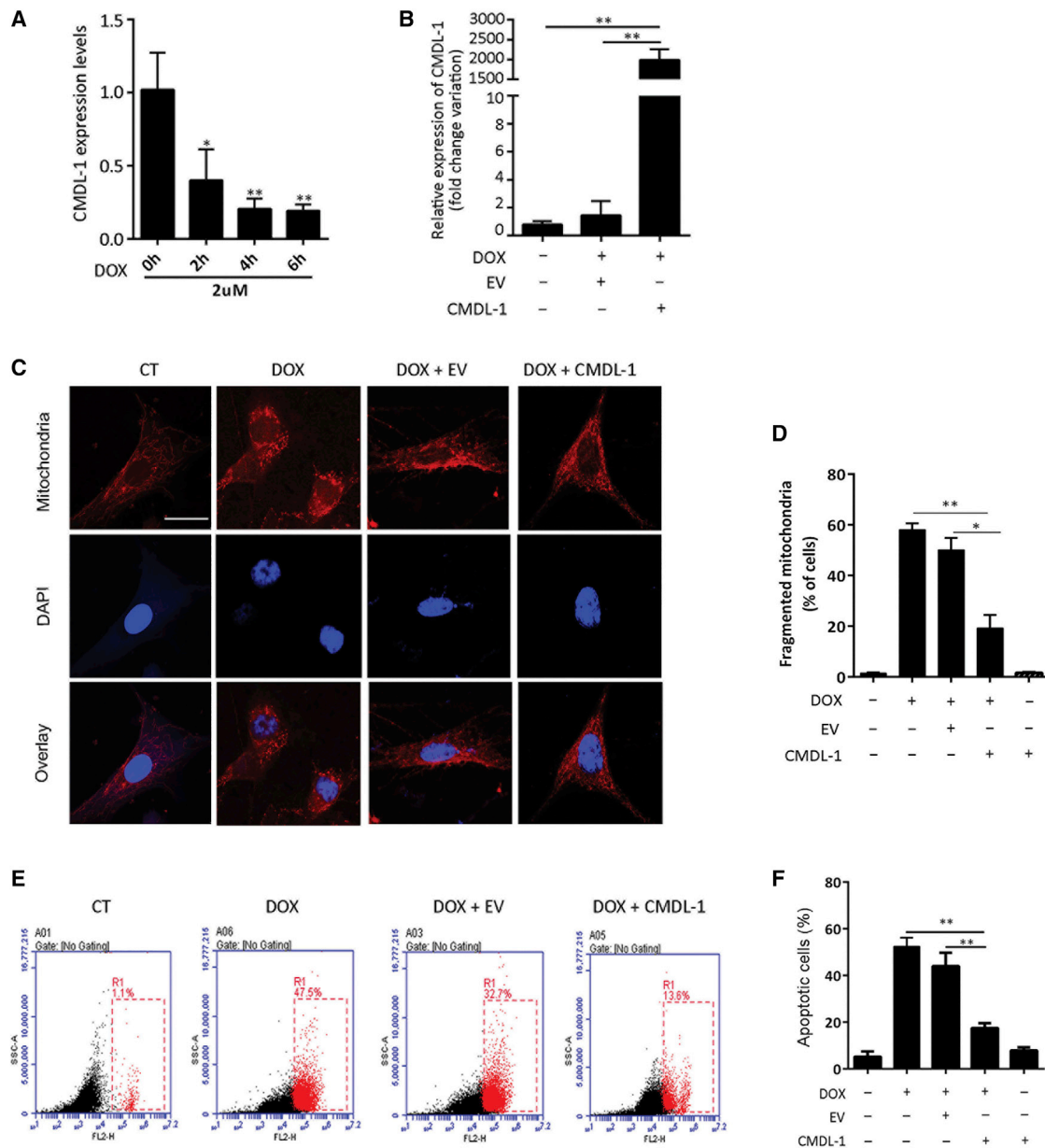
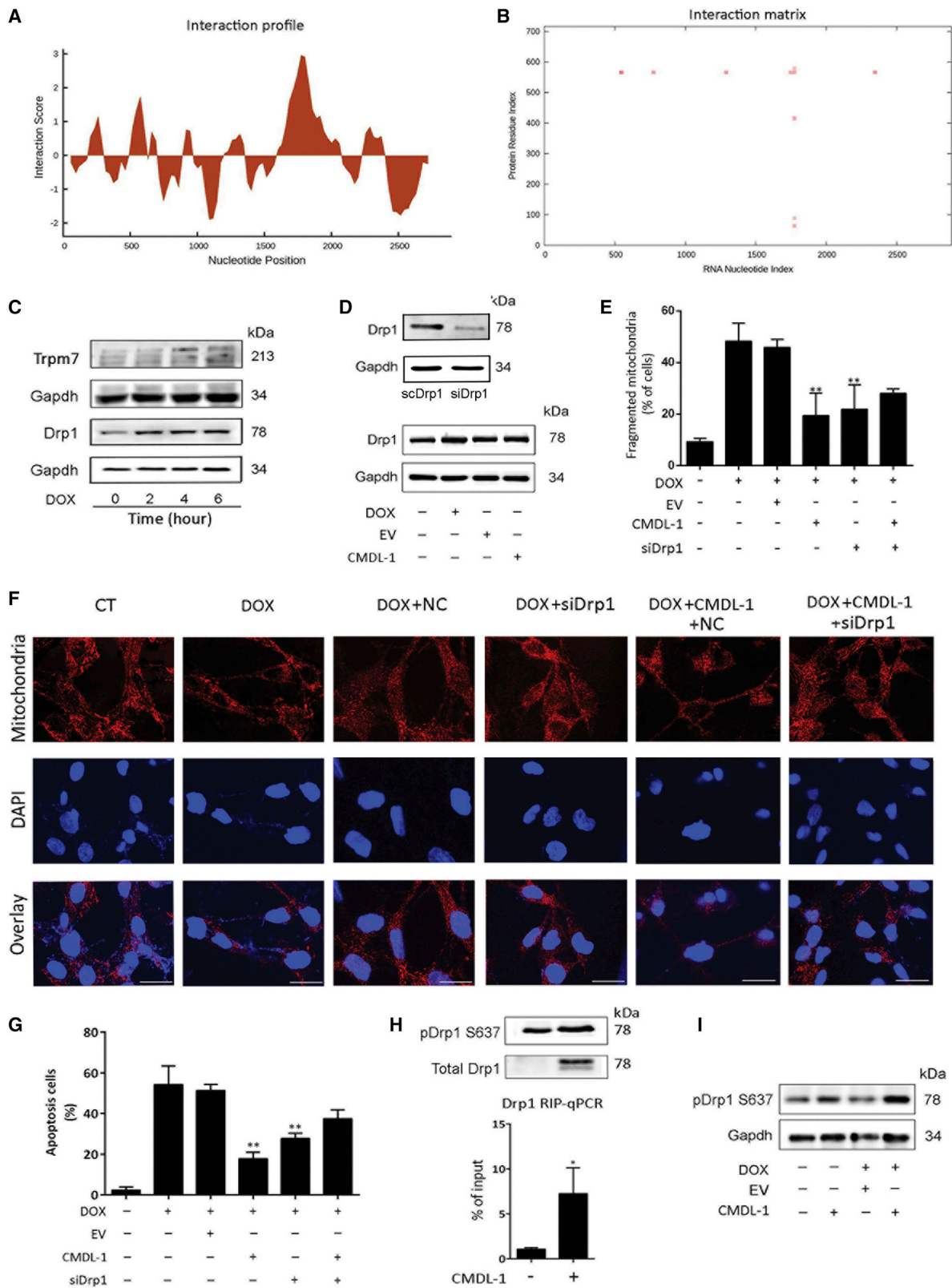


**Figure 5. Overexpression of CMDL-1 prevents the DOX-induced mitochondrial fission and apoptosis in cardiomyocytes**

(A) Dynamics of CMDL-1 expression at indicated durations of DOX exposure. \* $p < 0.05$ , \*\* $p < 0.01$  versus 0 h. (B) qPCR analysis of CMDL-1 expression. H9c2 cells were infected with CMDL-1 overexpressed virus and CMDL-1 expression was analyzed. (C and D) Overexpression of CMDL-1 ameliorates DOX-induced mitochondrial fission. Mitochondrial morphology (C) and quantification of mitochondrial fission (D) were analyzed after 6 h of DOX treatment. The disintegration levels of mitochondria (mitochondrial fission) in 250–300 cells were counted in 30–40 random fields using a confocal microscope. (E and F) Overexpression of CMDL-1 prevents DOX-induced apoptosis. (E) shows a representative flow cytometry plot, and (F) shows quantification of the dynamics of apoptosis in control (CT), DOX exposure, empty vector (EV) treated with DOX (DOX + EV), and CMDL-1 overexpression treated with DOX (DOX + CMDL-1) as analyzed by flow cytometry. Data presented are representative of at least three independent experiments. Data are expressed as the mean  $\pm$  SEM. \* $p < 0.05$ , \*\* $p < 0.01$ , \*\*\* $p < 0.001$ , one-way ANOVA.

Drp1 is a cytosolic protein, and phosphorylation at its serine 637 residue represses its activity, while dephosphorylation at the same residue can activate its function and induce mitochondrial fission.<sup>13</sup> Since CMDL-1 is located upstream to the protein kinase Trpm-7,

we hypothesized that CMDL-1 may regulate Drp1 phosphorylation. To answer this question, we performed RIP. IP analysis using anti-Drp1 and anti-phosphorylated (p-)Drp1 antibodies specific to the S637 site indicated that CMDL-1 overexpressed cells had increased



(legend on next page)

association with pDrp1, indicating that CMDL-1 may bind to p-Drp1 (Figure 6H). Additionally, we observed an increase in the S637 p-Drp1 level in CMDL-1 overexpressed cardiomyocytes after DOX exposure (Figure 6I). Moreover, the nuclear versus cytoplasmic expression analysis showed that a higher percentage of CMDL-1 was expressed in the cytoplasm compared to the nucleus, supporting the phenomenon that CMDL-1 could directly interact with Drp1 rather than controlling Drp1's transcription (Figure S2). These data collectively indicate that CMDL-1 can physically interact with Drp1.

#### **CMDL-1 expression is downregulated and apoptosis is increased in *in vivo* DOX-induced cardiac injury**

Then, we employed *in vivo* DOX-induced cardiac injury using adult rats. As shown in Figure 7A, we administered the indicated doses of DOX to the test group and equal volume of normal saline to the control group intraperitoneally to induce cardiotoxicity. Intraperitoneal injection was given once a week (cumulative total of 24 mg/kg) for 6 weeks, and the well-being of both control and test groups was closely monitored (Figure 7B). After 6 weeks, we analyzed the cardiac function using echocardiography. As shown in Figures 7C–7G, the DOX-exposed group showed a cardiac function reflected by all four cardiac echographic parameters, including a significant increase in left ventricular internal diameter at end systole (LVESd) and left ventricular internal diameter at end-diastole (LVEDd) with a significant decrease in left ventricular ejection fraction (LVEF) and left ventricular fractional shortening (LVFS). However, we did not observe statistically significant changes in cardiomyocyte cross-sectional area of DOX-exposed myocardium on wheat germ agglutinin (WGA) staining (Figures S3A and S3B). Next, we tested DOX-induced apoptosis in the heart tissue using TUNEL (terminal deoxynucleotidyl transferase dUTP nick-end labeling) staining and caspase-3 expression, and we observed a significant increase in TUNEL-positive cells (Figure 7H) and caspase-3 expression (Figure S4) in the DOX-exposed group compared to the control group. In addition, consistent with *in vitro* findings, we found that the expression of CMDL-1 was downregulated (Figure 7I). Collectively, we demonstrated that CMDL-1 prevents cardiac mitochondrial fission and apoptosis by regulating Drp1 phosphorylation.

## DISCUSSION

lncRNAs are emerging as crucial players in both cardiovascular physiology and pathology.<sup>25–27</sup> Increasing studies have supported the notion that they could serve as diagnostic biomarkers as well as therapeutic targets for cardiovascular diseases.<sup>28</sup> Our study, to our knowledge for the first time, deciphers the role of a novel lncRNA (CMDL-1) in the regulation of DOX cardiotoxicity. The expression of CMDL-1 is significantly downregulated in DOX-treated cardiomyocytes compared to untreated controls. Overexpression of CMDL-1 can enhance Drp1 phosphorylation at the S637 residue, leading to deactivation of Drp1 function and preventing DOX-induced mitochondrial fission and apoptosis, suggesting that CMDL-1 may serve as a therapeutic target in DOX cardiotoxicity.

As a paradox in cancer survivors, long-term anticancer treatment has been shown to induce delayed cardiotoxicity. Two categories of cardiotoxicity have been proposed, that is, type I, which is defined as permanent cardiotoxicity, and type II, which is considered reversible. Anthracycline group antineoplastic drugs, such as DOX, are linked to type I cardiotoxicity.<sup>29</sup> Although extensive research has been done on the optimal usage of DOX, its dose-dependent and cumulative cardiotoxicity remains the major concern for its long-term prescription in cancer patients.<sup>1,2</sup> Exploring the mechanism of DOX cardiotoxicity from the basics of lncRNA and mitochondrial dynamics might provide a novel therapeutic strategy for the treatment of DOX cardiotoxicity in cancer patients. It has been reported that DOX-induced free radical production is the primary mechanism causing myocardial injury because the heart is highly vulnerable to oxidative stress.<sup>5</sup> Reducing ROS production by using a late Na<sup>+</sup> current inhibitor, such as ranolazine, has been shown to blunt anthracycline-induced cardiac dysfunction.<sup>30</sup> The heart is an organ enriched with mitochondria, and mitochondria are the most extensively injured subcellular organelles during DOX cardiotoxicity. The dysfunctional mitochondria lead to structural changes such as mitochondrial swelling and myelin figures within mitochondria.<sup>31</sup> We and others have reported that DOX cardiotoxicity can induce mitochondrial fission and apoptosis, and the regulation of these pathways shows a significant reduction in cardiotoxicity<sup>9,21</sup> and cardiomyocyte loss.<sup>22</sup>

#### **Figure 6. CMDL-1 regulates apoptosis via Drp1**

(A and B) CMDL-1 is predicted to interact with Drp1. A positive interaction score indicates the predicted binding between CMDL-1 and Drp1 (A) and maps the CMDL-1 interaction domain to nucleotides 1500–2000 (B). RNA-protein interaction scores were generated using catRAPID software. (C) Drp1 and Trpm-7 expression levels. H9c2 cells were treated with DOX at the indicated time points, and cells were harvested for immunoblot analysis. (D) Immunoblot analysis of Drp1 expression level. Cells were transfected with siDrp1 to knock down Drp1 expression and with scrambled Drp1 (scDrp1) as CT for 24–72 h and harvested for immunoblot analysis (upper panel). Cells were infected with lentiviral overexpressing CMDL-1, and after 24 h they were harvested for immunoblot analysis (low panel). (E and F) CMDL-1 regulates mitochondrial fission via Drp1. Cells were transfected with EV, CMDL-1, and siDrp1 and exposed to DOX, and mitochondrial morphology was analyzed by confocal microscopy. (E) shows the quantification of mitochondrial fission. (F) shows representative mitochondrial morphology stained with MitoTracker red. \**p* < 0.05, \*\**p* < 0.01 versus DOX. Scale bars, 25 μm. (G) The anti-apoptotic effect of CMDL-1 decreases when Drp1 is minimally expressed (analyzed by flow cytometry). \**p* < 0.05, \*\**p* < 0.01 versus the DOX group. (H) Co-immunoprecipitation analysis. The upper panel shows western blot analysis of the specific association of Drp1 and p-Drp1 with CMDL-1. The lower panel shows Drp1 enrichment when CMDL-1 is overexpressed (analyzed by qPCR). IgG served as the negative CT. (I) CMDL-1 overexpression enhances the phosphorylation of Drp1 at the serine 637 residue. Data presented are representative of at least three independent experiments. Data are expressed as the mean ± SEM. \**p* < 0.05, \*\**p* < 0.01, one-way ANOVA.

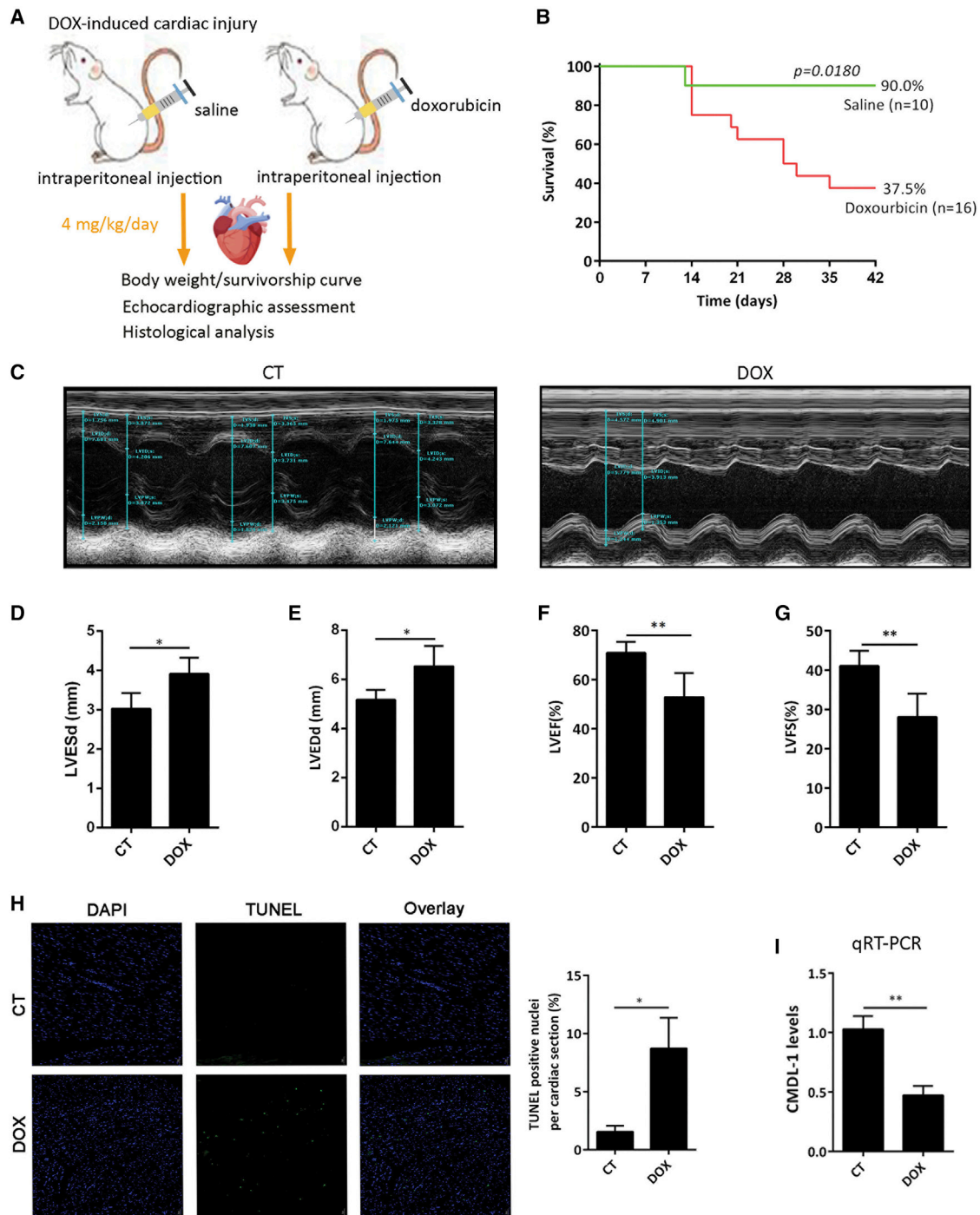


**Figure 7. In vivo analysis of CMDL-1 expression in DOX-induced cardiac injury**

(A) Schematic presentation of DOX-induced cardiac injury model. (B) Kaplan-Meier survival curves in CT and DOX-exposed rats. (C–G) The M-mode ultrasonic cardiography change of rat hearts detected by echocardiography in CT and test adult rats after 6 weeks of exposure of saline and DOX, respectively. The quantitative analyses of left ventricular internal diameter at end systole (LVESd; D), left ventricular internal diameter at end diastole (LVEDd; E), left ventricular ejection fraction (LVEF; F), and left ventricular fractional shortening (LVFS; G) are shown; n = 10 rats for CT and n = 16 rats for DOX. (H) TUNEL staining for apoptosis analysis. The left panel shows TUNEL staining, and the right panel shows quantification of apoptosis. (I) CMDL-1 expression between CT versus DOX-treated groups was analyzed by quantitative real-time PCR. Data presented are representative of at least three independent experiments. Data are expressed as the mean  $\pm$  SEM. \* $p < 0.05$ , \*\* $p < 0.01$ , two-tailed Student's t test.

Mitochondrial fission is involved in the development of progressive left ventricular hypertrophy and the development of cardiac failure.<sup>32,33</sup> Drp1 is the major mitochondrial fission protein,<sup>7</sup> and both *in vivo* and *in vitro* pulmonary arterial hypertensive rats showed increased Drp1-mediated mitochondrial fission.<sup>33</sup> Consistently, our study also showed that both *in vitro* and *in vivo* DOX cardiotoxicity induced the expression of Drp1. In transverse aortic banding (TAB)-treated mouse hearts and phenylephrine (PE)-treated rat neonatal cardiomyocytes, phosphorylation of Drp1 at serine 622 and translocation were observed.<sup>34</sup> The S637 of Drp1 is phosphorylated by protein kinase A (PKA),<sup>35</sup> Pim-1<sup>14</sup>, CaMKI- $\alpha$ ,<sup>36</sup> and ROCK1<sup>37</sup> depending on the type of stressed stimuli. Activation of Drp1 due to dephosphorylation at S637 induces Drp1 translocation to OMM and mitochondrial fission, leading to cell death.<sup>38</sup> Drp1 inhibitors exhibited cardioprotective effects evidenced by reducing ROS production, preserving mitochondrial morphology, and cytosolic calcium levels.<sup>12,33,39</sup> For example, administration of the Drp1 inhibitor P110 in adult rats with myocardial infarction (MI) resulted in a significant reduction in myocardial infarct size and left ventricular remodeling.<sup>39</sup> In addition, the administration of Drp1 inhibitors (mdivi-1 or P110) to both *in vivo* and *in vitro* pulmonary arterial hypertensive rats could prevent Drp1 translocation to mitochondria and inhibit mitochondrial fission, leading to preservation in right ventricular dysfunction.<sup>33</sup> In the present study, we observed that CMDL-1 could influence Drp1-mediated mitochondrial fission in DOX cardiotoxicity via regulating Drp1 phosphorylation. CMDL-1 promoted Drp1 S637 phosphorylation and inhibited Drp1 translocation to mitochondria, thereby preventing mitochondrial fission and apoptosis. During DOX cardiotoxicity, overexpression of CMDL-1 ameliorated DOX-induced cardiomyocyte loss, suggesting that CMDL-1 can be a potential therapeutic molecule in apoptosis-related cardiac injury.

lncRNAs are implicated in the regulation of diverse biological processes, including transcription, splicing, translation, chromosome gene dosage compensation, imprinting, epigenetic regulation, cell cycle control, cytoplasmic and nuclear trafficking, and cell differentiation.<sup>40</sup> Several recent studies have demonstrated that lncRNAs are involved in the pathogenesis of DOX cardiotoxicity via regulating apoptosis. Li et al.<sup>41</sup> reported that LINC00339 was markedly upregulated in DOX-induced cardiomyocytes and could aggravate apoptosis by targeting miR-484. Another study also found that cardiac hypertrophy-related factor (CHRF) was found to be upregulated in the heart in response to DOX.<sup>42</sup> CHRF inhibition prevented DOX-induced apoptosis and TGF- $\beta$ 1 expression by regulating the TGF- $\beta$ 1/Smads and TGF- $\beta$ /p38 pathways.<sup>42</sup> Of note, the function of lncRNAs can be varied depending on the type of cellular stress. lncRNA H19, which is highly expressed in myocardial tissue, plays an important role in apoptosis regulation. In diabetic cardiomyopathy (DCM) rat models induced by high glucose, H19 was significantly downregulated, and this reduction led to increased oxidative stress-induced apoptosis.<sup>43</sup> In contrast, Zhang et al.<sup>44</sup> showed that H19 expression was upregulated in rats with DOX (Adriamycin)-induced dilated cardiomyopathy (DCM), and overexpression of H19 was

associated with increased cardiomyocyte apoptosis. Although both studies observed that H19 exerts its function by sponging miR675, which consequently regulates the expression of anti-apoptosis gene PA2G4, whether H19 may function as either a pro-apoptotic or anti-apoptotic factor depends on the type of chemical stimuli, suggesting the complex role of lncRNAs in cardiac apoptotic pathways.

Recent studies indicated that lncRNAs exert their functions by regulating the phosphorylation of target signaling pathways. For instance, Zhou et al.<sup>45</sup> showed that in a rat model of diabetic cardiomyopathy, overexpression of lncRNA H19 epigenetically downregulated DIRAS3 expression and promoted mTOR phosphorylation, thereby inhibiting high glucose-induced cardiomyocyte autophagy. Similarly, lncRNA DANCR increased the phosphorylation of RXRA in the phosphatidylinositol 3-kinase (PI3K)/AKT signaling pathway and promoted tumorigenesis in patients with triple-negative breast cancer (TNBC). This study suggested that DANCR can be a pro-oncogene and can be a potential therapeutic target in treating TNBC.<sup>46</sup> In the present study, we found that CMDL-1 overexpression can prevent Drp1-mediated mitochondrial fission and apoptosis by directly interacting with Drp1 and enhancing its S637 phosphorylation. The full-length of CMDL-1 is poorly conserved across species, but the predicted protein-binding region with Drp1 is found to be conserved in mice and humans.

In summary, we profiled the differential expression of lncRNAs and mRNAs in DOX cardiotoxicity and identified a novel lncRNA named CMDL-1, which was downregulated in both *in vitro* and *in vivo* DOX cardiotoxicity. Our data indicated that CMDL-1 may function as an anti-apoptotic factor in the heart by targeting Drp1, particularly regulating Drp1 phosphorylation. However, the exact molecular mechanisms of CMDL-1 remain to be further verified in animal models. Collectively, our work highlights the less appreciated posttranslational mechanism of lncRNAs, modulating the phosphorylation status of its interacting proteins, and it also provides a fundamental piece of evidence for the therapeutic potential of CMDL-1 in the treatment of DOX cardiotoxicity.

## MATERIALS AND METHODS

### Cell culture and treatment

H9c2 cells were purchased from the Cell Bank of the Chinese Academy of Sciences (Beijing, China). H9c2 myoblast cells were cultured in Dulbecco's modified Eagle's medium (Gibco, Grand Island, NY, USA) supplemented with 10% fetal bovine serum (FBS) and 1% penicillin-streptomycin in a humidified atmosphere of 95% air and 5% CO<sub>2</sub> at 37°C. Cells were harvested by trypsinization and washed in phosphate-buffered saline (PBS). Cardiomyocytes were treated with 2  $\mu$ M DOX (Sigma, St. Louis, MO, USA) at the indicated time to induce cardiotoxicity.

### RNA extraction

Total RNA was extracted from the cells using TRIzol reagent (Invitrogen, USA) according to the manufacturer's instructions. RNA quantification and purification were measured by an ND-1000

spectrophotometer measuring absorbance ratios of A260/A280 and A260/A230, and RNA integrity was assessed by standard denaturing agarose gel electrophoresis.

#### RNA labeling and array hybridization

The expression of lncRNAs and mRNAs was determined using Arraystar rat lncRNA Microarray v2.0 (Arraystar, USA). Sample labeling and array hybridization were performed according to the Agilent one-color microarray-based gene expression analysis protocol (Agilent Technology, USA) with minor modifications for all samples. First, rRNA was removed from total RNA using an mRNA-only eukaryotic mRNA isolation kit (Epicenter Biotechnologies, USA). Then, each sample was amplified and transcribed into fluorescent cRNA along the entire length of the transcripts without 3' bias using the random priming method. The labeled cRNAs were purified using an RNeasy mini kit (QIAGEN, Germany) and then hybridized with the specific probes on the rat lncRNA array v2.0. Positive probes for housekeeping genes and negative probes were printed onto the array for quality control. The hybridized arrays were washed, fixed, and scanned with an Agilent DNA microarray scanner G2505C.

#### Microarray data analysis

Agilent feature extraction software (version 11.0.1.1) was used to analyze acquired array images. Quantile normalization and subsequent data processing were performed using the GeneSpring GX software package (version 12.1.1.0, Agilent Technologies). Differentially expressed lncRNAs and protein-coding mRNAs between the DOX-treated group and control groups were identified through volcano plot filtering (fold change > 2,  $p < 0.05$ ).

#### Functional group analysis

GO and KEGG pathway analysis were performed to clarify the function and biological process of differentially expressed lncRNAs and co-mRNAs from our microarray data. The differentially expressed mRNAs were annotated according to their attributes of gene products. GO was then used to assign the genes to different GO terms of their associated aspects, that is, biological processes, cellular components, and molecular functions, according to their annotations. Furthermore, the biological function of genes can be better understood via integrated analysis of KEGG pathways and gene annotations. The  $p$  value was used to determine the significance of the enrichment, and the false discovery rate (FDR) was used to evaluate the significance of the  $p$  value. The significant GO terms and pathways were filtered by  $p < 0.05$  and  $FDR < 0.05$ .

#### Quantitative real-time PCR

Quantitative real-time PCR was performed on a CFX96 real-time PCR detection system (Bio-Rad). Following the RNA extraction, 1  $\mu$ g of each RNA sample was reverse transcribed into cDNA using a PrimeScript RT reagent kit with a genomic DNA (gDNA) Eraser kit (Takara, Japan) according to the manufacturer's protocols. The quantitative real-time PCR system included 12.5  $\mu$ L of  $2\times$  SYBR Green (Takara, Japan), 1  $\mu$ L of primer (R/F), and 1  $\mu$ L of cDNA with DNAase/RNAase-free water up to 25  $\mu$ L. The lncRNA expres-

sion level was quantified based on the threshold cycle (Ct) values. GAPDH served as the internal control. The cycling parameters were as follows: 95°C for 30 s, followed by 40 cycles of 95°C for 5 s, 58°C or 60°C, 95°C for 15 s, 58°C or 60°C for 1 min, and 95°C for 15 s. The primers used for quantitative real-time PCR are shown in Table S1.

#### Adenoviral constructions and infection

The adenovirus overexpressing CMDL-1 was synthesized by Shanghai GeneChem. Cells were infected with the adenovirus containing CMDL-1 overexpressing vector according to the manufacturer's protocol. The CMDL-1 expression level was checked by quantitative real-time PCR.

#### Drp1 siRNA transfection

We purchased the Drp1 small interfering RNA (siRNA) and control siRNA-A (scrambled siRNA) from Santa Cruz Biotechnology (Dallas, TX, USA). Drp1 siRNA is a pool of three target-specific 19- to 25-nt siRNAs designed to knock down Drp1 gene expression, as we have described.<sup>47</sup> Briefly, cells were seeded 24 h before transfection and were then transfected with 30 nM scrambled siRNA or Drp1 siRNA using Lipofectamine 3000 reagent (Invitrogen, Carlsbad, CA, USA) per the manufacturer's instructions.

#### Apoptosis analysis (flow cytometry and TUNEL assay)

Cells were labeled with annexin V according to the manufacturer's instructions. Samples were analyzed with a flow cytometer (BD Accuri, BD Biosciences, USA), and the distribution of cells was determined using BD Biosciences software (BD Accuri C6). For apoptosis analysis, we used a TUNEL apoptosis detection kit (fluorescein isothiocyanate [FITC]) kit from Yeasen Biotech (Shanghai, China). After transfection and treatment, we rinsed, fixed, permeabilized, and stained the cells with the *in situ* 5-bromo-2'-deoxyuridine (BrdU)-red DNA fragmentation TUNEL assay according to the kit's instructions. We took images using a laser-scanning confocal microscope (Leica TCS SP8). For each group, we counted approximately 250–300 cells in 20–30 random fields. Results are expressed as percentages of TUNEL-positive cells.

#### Mitochondrial staining

We used MitoTracker red CMXRos (MitoSOX red mitochondrial superoxide indicator, Thermo Fisher Scientific, lot no. M36008) to stain the mitochondria of living cells. The cells were seeded onto the coverslips coated with 0.01% poly-L-lysine for 24 h. After various treatments, the cells were incubated with preheated MitoTracker red CMXRos staining fluid (0.02  $\mu$ M) for 25 min under normal conditions. The images of mitochondria were acquired using a laser-scanning confocal microscope (Leica TCS SP8). The percentage of mitochondria-disrupted cells relative to the total number of cells was expressed as mean  $\pm$  SEM. At least three separate experiments were performed and a minimum of 300 cells in each group were counted.

### Western blot analysis

After various treatments, cardiomyocytes were lysed by using the lysis buffer (150 mM NaCl, 1% Triton X-100, 1% sodium deoxycholate, 0.1% SDS) containing a mixture of protease inhibitors and keeping them on ice for 30 min. Equivalent amounts of proteins were loaded onto SDS-PAGE gel, and electrophoresis was carried out for 1.5 h at 150 V. Subsequently, the proteins were transferred from the gel to the polyvinylidene fluoride (PVDF) membrane, and the membrane was blocked with 5% skimmed milk powder in 1% Tris-buffered saline with Tween 20 (TBST) at room temperature for 1 h. The membranes were probed using primary antibodies, including the anti-Fis1 (1:1,000), anti-Drp1 (1:1,000), anti-caspase-3 (1:1,000), and anti-Gapdh (1:1,000) overnight at 4°C. Next, the membranes were washed five times with 1% TBST and incubated with secondary antibody prepared in 5% milk in 1% TBST for 1 h and then washed with 1% TBST. The blot images were captured by darkroom development using the chemiluminescence method.

### RIP analysis

RIP was performed using protein A/G plus agarose (Santa Cruz Biotechnology, catalog #sc-2003) according to the manufacturer's instructions. In brief, H9c2 cells treated as indicated were lysed in RIP lysis buffer, and the cell lysate was incubated with magnetic beads conjugated to anti Drp1 antibody (Cell Signaling Technology, catalog #8570S), p-Drp1 antibody (Cell Signaling Technology, catalog #4867, Ser367), or normal mouse immunoglobulin G (IgG). Co-precipitated RNAs were isolated, and Drp1 enrichment was analyzed by quantitative real-time PCR. Protein isolated by the beads was determined by western blot analysis.

### Animal experiments

Adult male SD rats (4 weeks old) were infused with DOX (4 mg/kg/day) to induce cardiac damage or the same volume of saline to the control group. All animal experiments were approved by the Institutional Review Board of Qingdao University, and the procedures were performed in accordance with the institutional guidelines of Qingdao University. The study was compliant with all relevant ethical regulations regarding animal research. Intraperitoneal injection was given once a week for 6 weeks, with a cumulative total of 24 mg/kg. All rats were subjected to echocardiographic measurements and hypertrophic analysis after 42 days.

### Histological analysis

Histological analysis of the hearts was carried out as we previously described.<sup>22</sup> Briefly, the hearts were excised and immediately fixed in 10% formalin. Subsequently, they were embedded in paraffin using a standard procedure, sectioned into 7- $\mu$ m slices, and stained with hematoxylin and eosin (H&E).

### Echocardiographic assessment of cardiac dimensions and function

Transthoracic echocardiography was performed using a Vevo 2100 imaging system (VisualSonics, Toronto, ON, Canada) with a real-time linear-array scan head (MS-450). Two-dimensional guided M-

mode tracing images were obtained in both parasternal long- and short-axis views at the level of papillary muscles. We obtained echocardiographic parameters, including LVESd, LVEDd, LVEF, and LVFS, which were calculated using the standard equations.<sup>22</sup> All measurements were averaged from at least three consecutive beats. After *in vivo* evaluation of cardiac function, the mice were killed and the hearts were harvested, weighed, and used for histological examination.

### Statistical analysis

The results are expressed as the mean  $\pm$  SEM of at least three independent experiments unless stated otherwise. Paired data were evaluated by a Student's *t* test. A one-way ANOVA was used for multiple comparisons. Statistical analyses were performed with GraphPad Prism 5.0 (GraphPad, San Diego, CA, USA). A *p* value of <0.05 was considered significant.

### SUPPLEMENTAL INFORMATION

Supplemental information can be found online at <https://doi.org/10.1016/j.omtn.2021.08.006>.

### ACKNOWLEDGMENTS

This work was supported by the Natural Science Foundation of Shandong Province (ZR2019BH014) and the National Natural Science Foundation of China (82050410450, 81850410551, and 91849209). This study was approved by the Ethical Review Board of the Affiliated Hospital of Qingdao University, College of Medicine, Qingdao University.

### AUTHOR CONTRIBUTIONS

L.H.H.A. conceived and designed the study. L.H.H.A., X.C., Z.L., S.-y.W., C.Z., and Z.-q.L. performed the experiments. L.H.H.A. and X.C. wrote the manuscript. L.H.H.A., J.C.C.J., Y.W., and P.L. analyzed the data, edited, and submitted the manuscript. All authors discussed and finalized the manuscript for submission.

### DECLARATION OF INTERESTS

The authors declare no competing interests.

### REFERENCES

1. Singal, P.K., and Iliskovic, N. (1998). Doxorubicin-induced cardiomyopathy. *N. Engl. J. Med.* 339, 900–905.
2. Thorn, C.F., Oshiro, C., Marsh, S., Hernandez-Boussard, T., McLeod, H., Klein, T.E., and Altman, R.B. (2011). Doxorubicin pathways: Pharmacodynamics and adverse effects. *Pharmacogenet. Genomics* 21, 440–446.
3. Mele, D., Tocchetti, C.G., Pagliaro, P., Madonna, R., Novo, G., Pepe, A., Zito, C., Maurea, N., and Spallarossa, P. (2016). Pathophysiology of anthracycline cardiotoxicity. *J. Cardiovasc. Med. (Hagerstown)* 17 (Suppl 1), e3–e11.
4. Green, P.S., and Leeuwenburgh, C. (2002). Mitochondrial dysfunction is an early indicator of doxorubicin-induced apoptosis. *Biochim. Biophys. Acta* 1588, 94–101.
5. Octavia, Y., Tocchetti, C.G., Gabrielson, K.L., Janssens, S., Crijns, H.J., and Moens, A.L. (2012). Doxorubicin-induced cardiomyopathy: From molecular mechanisms to therapeutic strategies. *J. Mol. Cell. Cardiol.* 52, 1213–1225.
6. Zhang, Y.W., Shi, J., Li, Y.J., and Wei, L. (2009). Cardiomyocyte death in doxorubicin-induced cardiotoxicity. *Arch. Immunol. Ther. Exp. (Warsz.)* 57, 435–445.

7. Nan, J., Zhu, W., Rahman, M.S., Liu, M., Li, D., Su, S., Zhang, N., Hu, X., Yu, H., Gupta, M.P., and Wang, J. (2017). Molecular regulation of mitochondrial dynamics in cardiac disease. *Biochim. Biophys. Acta Mol. Cell Res.* 1864, 1260–1273.
8. Marín-García, J., and Akhmedov, A.T. (2016). Mitochondrial dynamics and cell death in heart failure. *Heart Fail. Rev.* 21, 123–136.
9. Catanzaro, M.P., Weiner, A., Kaminaris, A., Li, C., Cai, F., Zhao, F., Kobayashi, S., Kobayashi, T., Huang, Y., Sesaki, H., and Liang, Q. (2019). Doxorubicin-induced cardiomyocyte death is mediated by unchecked mitochondrial fission and mitophagy. *FASEB J.* 33, 11096–11108.
10. Fonseca, T.B., Sánchez-Guerrero, Á., Milosevic, I., and Raimundo, N. (2019). Mitochondrial fission requires Drp1 but not dynamins. *Nature* 570, E34–E42.
11. Taguchi, N., Ishihara, N., Jofuku, A., Oka, T., and Mihara, K. (2007). Mitotic phosphorylation of dynamin-related GTPase Drp1 participates in mitochondrial fission. *J. Biol. Chem.* 282, 11521–11529.
12. Sharp, W.W. (2015). Dynamin-related protein 1 as a therapeutic target in cardiac arrest. *J. Mol. Med. (Berl.)* 93, 243–252.
13. Cereghetti, G.M., Stangherlin, A., Martins de Brito, O., Chang, C.R., Blackstone, C., Bernardi, P., and Scorrano, L. (2008). Dephosphorylation by calcineurin regulates translocation of Drp1 to mitochondria. *Proc. Natl. Acad. Sci. USA* 105, 15803–15808.
14. Din, S., Mason, M., Völkers, M., Johnson, B., Cottage, C.T., Wang, Z., Joyo, A.Y., Quijada, P., Erhardt, P., Magnuson, N.S., et al. (2013). Pim-1 preserves mitochondrial morphology by inhibiting dynamin-related protein 1 translocation. *Proc. Natl. Acad. Sci. USA* 110, 5969–5974.
15. Shen, S., Jiang, H., Bei, Y., Xiao, J., and Li, X. (2017). Long non-coding RNAs in cardiac remodeling. *Cell. Physiol. Biochem.* 41, 1830–1837.
16. Haemmmig, S., Simion, V., Yang, D., Deng, Y., and Feinberg, M.W. (2017). Long non-coding RNAs in cardiovascular disease, diagnosis, and therapy. *Curr. Opin. Cardiol.* 32, 776–783.
17. Viereck, J., and Thum, T. (2017). Circulating noncoding RNAs as biomarkers of cardiovascular disease and injury. *Circ. Res.* 120, 381–399.
18. Wang, K., Long, B., Zhou, L.Y., Liu, F., Zhou, Q.Y., Liu, C.Y., Fan, Y.Y., and Li, P.F. (2014). CARL lncRNA inhibits anoxia-induced mitochondrial fission and apoptosis in cardiomyocytes by impairing miR-539-dependent PHB2 downregulation. *Nat. Commun.* 5, 3596.
19. Wang, K., Sun, T., Li, N., Wang, Y., Wang, J.X., Zhou, L.Y., Long, B., Liu, C.Y., Liu, F., and Li, P.F. (2014). MDRL lncRNA regulates the processing of miR-484 primary transcript by targeting miR-361. *PLoS Genet.* 10, e1004467.
20. Tian, T., Lv, X., Pan, G., Lu, Y., Chen, W., He, W., Lei, X., Zhang, H., Liu, M., Sun, S., et al. (2019). Long noncoding RNA MPRL promotes mitochondrial fission and cisplatin chemosensitivity via disruption of pre-miRNA processing. *Clin. Cancer Res.* 25, 3673–3688.
21. Osataphan, N., Phrommintikul, A., Chattipakorn, S.C., and Chattipakorn, N. (2020). Effects of doxorubicin-induced cardiotoxicity on cardiac mitochondrial dynamics and mitochondrial function: Insights for future interventions. *J. Cell. Mol. Med.* 24, 6534–6557.
22. Zhou, L., Li, R., Liu, C., Sun, T., Htet Aung, L.H., Chen, C., Gao, J., Zhao, Y., and Wang, K. (2017). Foxo3a inhibits mitochondrial fission and protects against doxorubicin-induced cardiotoxicity by suppressing MIEF2. *Free Radic. Biol. Med.* 104, 360–370.
23. Losón, O.C., Song, Z., Chen, H., and Chan, D.C. (2013). Fis1, Mff, MiD49, and MiD51 mediate Drp1 recruitment in mitochondrial fission. *Mol. Biol. Cell* 24, 659–667.
24. Otera, H., Wang, C., Cleland, M.M., Setoguchi, K., Yokota, S., Youle, R.J., and Mihara, K. (2010). Mff is an essential factor for mitochondrial recruitment of Drp1 during mitochondrial fission in mammalian cells. *J. Cell Biol.* 191, 1141–1158.
25. Bär, C., Chatterjee, S., and Thum, T. (2016). Long noncoding RNAs in cardiovascular pathology, diagnosis, and therapy. *Circulation* 134, 1484–1499.
26. Wang, Y., and Sun, X. (2020). The functions of lncRNA in the heart. *Diabetes Res. Clin. Pract.* 168, 108249.
27. Han, P., Li, W., Lin, C.-H., Yang, J., Shang, C., Nuernberg, S.T., Jin, K.K., Xu, W., Lin, C.-Y., Lin, C.-J., et al. (2014). A long noncoding RNA protects the heart from pathological hypertrophy. *Nature* 514, 102–106.
28. Wu, T., and Du, Y. (2017). lncRNAs: From basic research to medical application. *Int. J. Biol. Sci.* 13, 295–307.
29. Riccio, G., Coppola, C., Piscopo, G., Capasso, I., Maurea, C., Esposito, E., De Lorenzo, C., and Maurea, N. (2016). Trastuzumab and target-therapy side effects: Is still valid to differentiate anthracycline type I from type II cardiomyopathies? *Hum. Vaccin. Immunother.* 12, 1124–1131.
30. Riccio, G., Antonucci, S., Coppola, C., D'Avino, C., Piscopo, G., Fiore, D., Maurea, C., Russo, M., Rea, D., Arra, C., et al. (2018). Ranolazine attenuates trastuzumab-induced heart dysfunction by modulating ROS production. *Front. Physiol.* 9, 38.
31. Cole, M.P., Chaiswing, L., Oberley, T.D., Edelmann, S.E., Piascik, M.T., Lin, S.M., Kinningham, K.K., and St Clair, D.K. (2006). The protective roles of nitric oxide and superoxide dismutase in adriamycin-induced cardiotoxicity. *Cardiovasc. Res.* 69, 186–197.
32. Givvimani, S., Pushpakumar, S., Veeranki, S., and Tyagi, S.C. (2014). Dysregulation of Mfn2 and Drp-1 proteins in heart failure. *Can. J. Physiol. Pharmacol.* 92, 583–591.
33. Tian, L., Neuber-Hess, M., Mewburn, J., Dasgupta, A., Dunham-Snary, K., Wu, D., Chen, K.H., Hong, Z., Sharp, W.W., Kutty, S., and Archer, S.L. (2017). Ischemia-induced Drp1 and Fis1-mediated mitochondrial fission and right ventricular dysfunction in pulmonary hypertension. *J. Mol. Med. (Berl.)* 95, 381–393.
34. Chang, Y.W., Chang, Y.T., Wang, Q., Lin, J.J., Chen, Y.J., and Chen, C.C. (2013). Quantitative phosphoproteomic study of pressure-overloaded mouse heart reveals dynamin-related protein 1 as a modulator of cardiac hypertrophy. *Mol. Cell. Proteomics* 12, 3094–3107.
35. Cribbs, J.T., and Strack, S. (2007). Reversible phosphorylation of Drp1 by cyclic AMP-dependent protein kinase and calcineurin regulates mitochondrial fission and cell death. *EMBO Rep.* 8, 939–944.
36. Han, X.J., Lu, Y.F., Li, S.A., Kaitsuka, T., Sato, Y., Tomizawa, K., Nairn, A.C., Takei, K., Matsui, H., and Matsushita, M. (2008). CaM kinase  $\alpha$ -induced phosphorylation of Drp1 regulates mitochondrial morphology. *J. Cell Biol.* 182, 573–585.
37. Wang, W., Wang, Y., Long, J., Wang, J., Haudek, S.B., Overbeek, P., Chang, B.H., Schumacker, P.T., and Danesh, F.R. (2012). Mitochondrial fission triggered by hyperglycemia is mediated by ROCK1 activation in podocytes and endothelial cells. *Cell Metab.* 15, 186–200.
38. Sharp, W.W., Fang, Y.H., Han, M., Zhang, H.J., Hong, Z., Banathy, A., Morrow, E., Ryan, J.J., and Archer, S.L. (2014). Dynamin-related protein 1 (Drp1)-mediated diastolic dysfunction in myocardial ischemia-reperfusion injury: therapeutic benefits of Drp1 inhibition to reduce mitochondrial fission. *FASEB J.* 28, 316–326.
39. Disatnik, M.H., Ferreira, J.C., Campos, J.C., Gomes, K.S., Dourado, P.M., Qi, X., and Mochly-Rosen, D. (2013). Acute inhibition of excessive mitochondrial fission after myocardial infarction prevents long-term cardiac dysfunction. *J. Am. Heart Assoc.* 2, e000461.
40. Patil, V.S., Zhou, R., and Rana, T.M. (2014). Gene regulation by non-coding RNAs. *Crit. Rev. Biochem. Mol. Biol.* 49, 16–32.
41. Li, J., Li, L., Li, X., and Wu, S. (2018). Long noncoding RNA LINC00339 aggravates doxorubicin-induced cardiomyocyte apoptosis by targeting miR-484. *Biochem. Biophys. Res. Commun.* 503, 3038–3043.
42. Chen, L., Yan, K.P., Liu, X.C., Wang, W., Li, C., Li, M., and Qiu, C.G. (2018). Valsartan regulates TGF- $\beta$ /Smads and TGF- $\beta$ /p38 pathways through lncRNA CHRFB to improve doxorubicin-induced heart failure. *Arch. Pharm. Res.* 41, 101–109.
43. Li, X., Wang, H., Yao, B., Xu, W., Chen, J., and Zhou, X. (2016). lncRNA H19/miR-675 axis regulates cardiomyocyte apoptosis by targeting VDAC1 in diabetic cardiomyopathy. *Sci. Rep.* 6, 36340.
44. Zhang, Y., Zhang, M., Xu, W., Chen, J., and Zhou, X. (2017). The long non-coding RNA H19 promotes cardiomyocyte apoptosis in dilated cardiomyopathy. *Oncotarget* 8, 28588–28594.
45. Zhuo, C., Jiang, R., Lin, X., and Shao, M. (2017). lncRNA H19 inhibits autophagy by epigenetically silencing of DIRAS3 in diabetic cardiomyopathy. *Oncotarget* 8, 1429–1437.
46. Tang, J., Zhong, G., Zhang, H., Yu, B., Wei, F., Luo, L., Kang, Y., Wu, J., Jiang, J., Li, Y., et al. (2018). lncRNA DANCER upregulates PI3K/AKT signaling through activating serine phosphorylation of RXRA. *Cell Death Dis.* 9, 1167.
47. Aung, L.H.H., Li, R., Prabhakar, B.S., and Li, P. (2017). Knockdown of Mtfp1 can minimize doxorubicin cardiotoxicity by inhibiting Dnm1l-mediated mitochondrial fission. *J. Cell. Mol. Med.* 21, 3394–3404.